

How mutations in tRNA distant from the anticodon affect the fidelity of decoding

T Martin Schmeing¹⁻³, Rebecca M Voorhees^{1,3}, Ann C Kelley¹ & V Ramakrishnan¹

The ribosome converts genetic information into protein by selecting aminoacyl tRNAs whose anticodons base-pair to an mRNA codon. Mutations in the tRNA body can perturb this process and affect fidelity. The Hirsh suppressor is a well-studied tRNA^{Trp} harboring a G24A mutation that allows readthrough of UGA stop codons. Here we present crystal structures of the 70S ribosome complexed with EF-Tu and aminoacyl tRNA (native tRNA^{Trp}, G24A tRNA^{Trp} or the miscoding A9C tRNA^{Trp}) bound to cognate UGG or near-cognate UGA codons, determined at 3.2-Å resolution. The A9C and G24A mutations lead to miscoding by facilitating the distortion of tRNA required for decoding. A9C accomplishes this by increasing tRNA flexibility, whereas G24A allows the formation of an additional hydrogen bond that stabilizes the distortion. Our results also suggest that each native tRNA will adopt a unique conformation when delivered to the ribosome that allows accurate decoding.

The elucidation of the genetic code in the 1960s revealed that each three-nucleotide mRNA sequence coded for a particular amino acid and that this code determines the primary sequence of proteins. It was discovered that these codons are recognized by a complementary tRNA anticodon, which is covalently linked to the appropriate amino acid. Though tRNAs were initially assumed to be inert adaptor molecules, the discovery that a mutation (G24A) in the D-stem of tRNA^{Trp} allows suppression of UGA stop codons changed this view. G24 is far from the anticodon (Fig. 1a), so this mutation demonstrated that properties of the tRNA body are also critical for decoding¹. G24 pairs with U11, so it is even more puzzling why its mutation to A24, which could form a canonical base pair with U11, would affect fidelity. Also, the strength of the base 24–base 11 pair does not correlate with miscoding efficiency².

Since the identification of this so-called Hirsh suppressor tRNA (from here on referred to as G24A tRNA^{Trp}), several other mutations in tRNA^{Trp} outside the anticodon have been shown to lead to miscoding, including A9C³⁻⁵. Four decades of biochemical and kinetic experiments have attempted to explain in detail how such mutations in the tRNA body cause miscoding^{2,3,5-7}. These studies have led to many conflicting theories, including that the G24A mutation alters the tRNA flexibility^{6,7}, changes internal base-pairing in the tRNA² or allows additional interactions between the tRNA and the ribosome^{5,7}. It is likely that these mutations affect the ability of tRNA to adopt the distorted A/T conformation during decoding, which allows the tRNA to continue to interact with elongation factor Tu (EF-Tu) while base-pairing with the codon at the decoding center. However, detailed structures of these mutant tRNAs trapped during decoding on the ribosome are needed to provide a molecular understanding of their loss of fidelity. This information will also provide insight into the native mechanisms used by the translation machinery to ensure accurate decoding.

Native tRNA^{Trp} recognizes only its cognate UGG codon efficiently. However, both A9C and G24A mutations in tRNA^{Trp} allows the aberrant

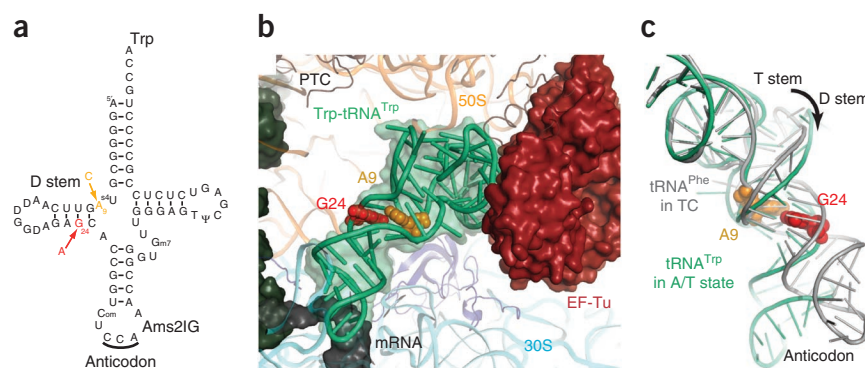
recognition of the near-cognate UGA stop codon. Discrimination between UGA and UGG requires differentiation between an A and G at the wobble position, where Watson-Crick base-pairing is not stringently monitored⁸. tRNA^{Trp} is the only elongator tRNA that discriminates between purines in the wobble position without the aid of a modification at residue 34 (ref. 9), and UGA has a readthrough rate as high as 10⁻² compared to the more typical ribosomal error rate of 10⁻³–10⁻⁴ (refs. 10,11). Furthermore, G24A and A9C tRNA^{Trp} are ~8- and 18-fold better, respectively, at recognizing UGA than wild-type tRNA^{Trp} (ref. 2). Additionally, although GTP hydrolysis by EF-Tu should only be efficiently triggered by binding to a cognate codon, the rate of GTPase activation is fivefold faster with G24A tRNA^{Trp} on a noncognate codon as it is with wild-type tRNA⁷. The rate of GTPase activation by G24A tRNA on a stop codon is only half that of native tRNA^{Trp} on its cognate codon. Therefore, the energetic difference between binding of the G24A and native tRNA^{Trp} to a near-cognate codon is on the order of 4 kJ mol⁻¹, approximately the energy of a single additional hydrogen bond under solvated conditions¹².

During decoding, the combined energetic penalty of inducing the conformational changes required in the 30S subunit, the tRNA (A/T state) and EF-Tu is precisely balanced against the energy derived from cognate tRNA binding. This includes contributions from the interaction of 16S ribosomal RNA nucleotides A1492, A1493 and G530 with the minor groove of the codon-anticodon helix. Mutations in the tRNA body could cause miscoding through two possible mechanisms: by increasing the flexibility of the tRNA body or by forming stabilizing interactions in the A/T state. Both strategies lower the energetic penalty for adoption of the A/T conformation that is required for GTPase activation. With the goal of understanding the error-prone phenotypes of both the G24A and A9C tRNA^{Trp}, we have solved four crystal structures of aminoacyl tRNAs bound with EF-Tu

¹MRC Laboratory of Molecular Biology, Cambridge, UK. ²Present address: Biochemistry Department, McGill University, Montreal, Quebec, Canada. ³These authors contributed equally to this work. Correspondence should be addressed to T.M.S. (martin.schmeing@mcgill.ca).

Received 19 October 2010; accepted 8 December 2010; published online 6 March 2011; doi:10.1038/nsmb.2003

Figure 1 Overview of miscoding mutations and Trp-tRNA^{Trp} bound in the A/T state. (a) The traditional cloverleaf diagram of Trp-tRNA^{Trp} showing the locations of the miscoding mutations A9C (orange) and G24A (red). (b) When bound to the ribosome along with EF-Tu, the aminoacyl tRNA (green) adopts the distorted A/T conformation. Structures were also determined for Trp-tRNA^{Trp} containing mutations at position 24 (red spheres) and 9 (orange spheres). (c) The A/T conformation requires a ~30° bend in the tRNA body (green) compared to a canonical tRNA (gray)¹⁹. This bend is achieved through two isolated regions of distortion, first in the anticodon stem and the second in the D-stem, where both the A9C and G24A mutations are located.



to the 70S ribosome from *Thermus thermophilus* and stabilized by the antibiotic kirromycin. These four structures contain (i) wild-type Trp-tRNA^{Trp} bound to the cognate UGG codon, (ii) G24A Trp-tRNA^{Trp} bound to UGG, (iii) G24A Trp-tRNA^{Trp} bound to the near-cognate UGA stop codon and (iv) A9C Trp-tRNA^{Trp} bound to UGA (Fig. 1, Table 1). The structures reveal the detailed mechanisms by which the G24A and A9C mutations lead to miscoding. Furthermore, a comparison with the structure of 70S-EF-Tu-Thr-tRNA^{Thr} demonstrates how different tRNAs use distinct conformations to productively bind to the ribosome and thereby ensure accurate decoding.

RESULTS

The overall conformation of ribosomal decoding complexes

Codon selection by the ribosome triggers GTP hydrolysis; a ribosomal complex stalled at the point of GTP hydrolysis would thus provide the best structural insight into decoding. Comparison of the structures of the ternary complex on the ribosome directly before (stalled by a GTP analog)¹³ and after (stalled by kirromycin, this study) GTP hydrolysis reveals an identical tRNA conformation (Supplementary Fig. 1). Therefore, although the kirromycin-stalled structures presented here represent post-hydrolysis complexes, the observed conformations of the tRNA body are indeed relevant for understanding how the G24A and A9C mutations affect tRNA selection. All complexes reported here have Watson-Crick base pairs in the first two positions of the codon-anticodon helix, so the 16S rRNA residues A1492–3 and G530, which monitor these positions, are flipped out and the 30S subunit is in the ‘closed’ conformation. The conformational changes predicted to communicate codon matching from the ribosome to EF-Tu are observed, though some movements are less pronounced¹⁴. The G24A and A9C mutations do not appear to alter the interactions between tRNA^{Trp} and the ribosome, in contrast to a recent hypothesis^{5,7}. Despite these similarities, changes observed at the anticodon and functionally important differences in the tRNA body suggest a solution to these decades-old miscoding puzzles.

The decoding center

For both the G24A and A9C tRNAs bound to the UGA stop codon, a clear C34-A3 mismatch is observed at the wobble position (Fig. 2a,b). Formation of this hydrogen bonding interaction results in shifts in both the tRNA anticodon and mRNA codon. This distortion is propagated along the tRNA body through residue 31 (Fig. 2c,d).

Wild-type and mutant tRNA^{Trp} in the A/T conformation

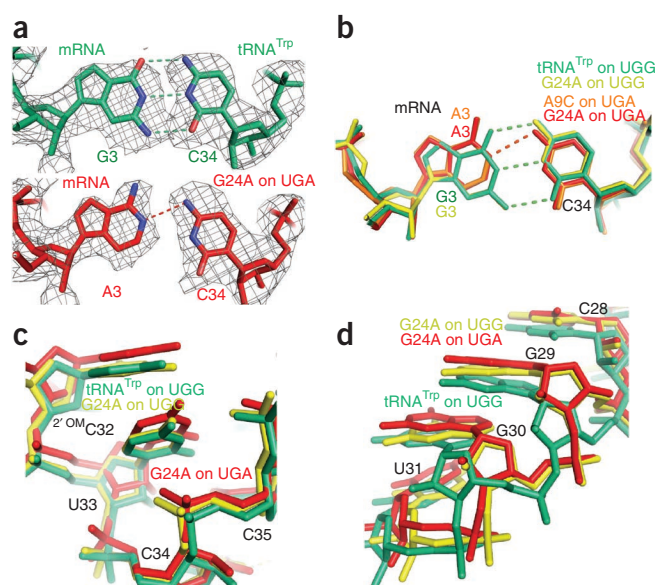
Outside the decoding center, the structure of Trp-tRNA^{Trp} is distorted to maintain interactions with EF-Tu (Fig. 1b,c)¹⁴. The bodies of the wild-type and mutant tRNAs Trp-tRNA^{Trp} are in a very similar conformation compared to one another and to Thr-tRNA^{Thr} (ref. 14). However, in all Trp-tRNA^{Trp} studied here, the phosphodiester backbone of residues 44–45 is positioned closely into the tRNA body, near residues 25–26 (Fig. 3).

Table 1 Summary of crystallographic data and refinement

	70S-EF-Tu-Trp-tRNA ^{Trp} (merged from 5 crystals)	70S-EF-Tu-G24A-Trp-tRNA ^{Trp} UGG (from 2 crystals)	70S-EF-Tu-G24A-Trp-tRNA ^{Trp} UGA (from 2 crystals)	70S-EF-Tu-A9C-Trp-tRNA ^{Trp} UGA (from 2 crystals)
Data collection				
Space group	<i>P</i> 2 ₁	<i>P</i> 2 ₁	<i>P</i> 2 ₁	<i>P</i> 2 ₁
Cell dimensions <i>a</i> , <i>b</i> , <i>c</i> (Å)	290.2, 269.2, 404.0	289.8, 269.1, 404.0	289.9, 269.4, 404.5	289.9, 268.5, 403.6
α , β , γ (°)	90.0, 91.5, 90.0	90.0, 91.2, 90.0	90.0, 91.5, 90.0	90.0, 91.6, 90.0
Resolution (Å)	50–3.1 (3.2–3.1) ^a	50–3.1 (3.2–3.1) ^b	50–3.1 (3.2–3.1) ^c	50–3.1 (3.2–3.1) ^d
<i>R</i> _{sym}	19.9 (115.2)	20.4 (100.9)	26.8 (130.1)	21.5 (103.3)
<i>I</i> / σ	7.12 (1.24) ^a	7.27 (1.35) ^b	6.19 (1.23) ^c	10.48 (1.69) ^d
Completeness (%)	99.8 (99.9)	97.4 (92.7)	98.7 (98.5)	97.9 (93.2)
Redundancy	6.3 (5.2)	4.6 (4.1)	6.4 (6.5)	5.0 (4.4)
Refinement				
Resolution (Å)	50.0–3.1	50.0–3.1	50.0–3.1	50.0–3.1
No. unique reflections	1,116, 606	1,087, 126	1,105, 502	1,090, 696
<i>R</i> _{work} / <i>R</i> _{free}	23.7/26.4	24.7/28.5	23.8/27.5	24.3/26.7
No. atoms				
RNA	205, 448	205, 202	205, 200	205, 442
Protein	100, 888	100, 888	100, 888	100, 888
B-factors				
RNA	99	82	90	76
Protein	103	86	92	81
R.m.s. deviations				
Bond lengths (Å)	0.008	0.008	0.008	0.007
Bond angles (°)	1.2	1.3	1.3	1.2

^a*I*/ σ = 1.97 at 3.2 Å resolution. ^b*I*/ σ = 2.08 at 3.2 Å resolution. ^c*I*/ σ = 1.92 at 3.2 Å resolution. ^d*I*/ σ = 2.58 at 3.2 Å resolution.

Figure 2 Comparison of cognate and near-cognate structures in the decoding center. (a) Unbiased $F_o - F_c$ electron density (shown at 1.3σ within 2 \AA of EF-Tu) is shown for residues in the wobble position of the codon-anticodon helix. (b) Binding of a near-cognate tRNA (A9C on UGA, orange; G24A on UGA, red), compared to a cognate tRNA (G24A on UGG, yellow; tRNA^{Trp} on UGG, green) results in a shift in both the tRNA anticodon and mRNA codon. (c) The distortion in the anticodon caused by this mismatch is propagated three residues, resulting in a shift in the tRNA backbone for the G24A on UGA when compared to the G24A or tRNA^{Trp} on UGG. (d) This distortion does not, however, continue past residue 31; by residue 28, the backbone of the G24A on UGA has converged with that of the G24A on UGG.



The structures of G24A tRNA^{Trp} bound to both the UGG and UGA codons indicate that the mutation at residue 24 allows formation of an additional hydrogen bond in the A/T conformation. In both structures, the N6 of nucleotide A24, which is not present in the wild-type G24, is within hydrogen bonding distance of the exocyclic O6 of G44 (Fig. 3a).

Conversely, the structure of A9C tRNA^{Trp} bound to a UGA codon shows that this mutation disrupts hydrogen bonding in the A/T conformation. In wild-type tRNA^{Trp}, a base triple is formed between residues A9–A23–U12. When residue A9 is mutated to cytosine, this base triple is weaker, as a cytidine is unable to form the two hydrogen bonds provided by adenosine (Fig. 3c).

DISCUSSION

Conformational changes in the decoding center

One noteworthy difference between the four complexes is at the decoding center where a C34·A3 mismatch is observed in the wobble position for both the G24A and A9C tRNAs bound to the UGA stop codon (Fig. 2a,b). In both cases, C34 in the tRNA anticodon and A3 in the mRNA codon each shift to facilitate this interaction. This is in contrast to previous studies in which the mRNA remained stationary while interacting with several cognate anticodons¹⁵. The distortion at the anticodon required for binding near-cognate UGA is propagated three residues, causing a shift in the G24A and A9C tRNAs between residues 34–31 (Fig. 2c). Mutations in this region are known to cause miscoding¹⁶, perhaps by altering the anticodon stem to allow binding to a mismatched codon. However, this movement is not communicated to the rest of the tRNA, as after residue 31 the structures of the G24A tRNA in the near-cognate and cognate complexes converge. The error-prone phenotype of the G24A and A9C tRNAs is therefore

not caused by a distortion propagated from the anticodon but rather is a direct effect of these mutations on the tRNA body. This is consistent with kinetic data that show a similar increase in the rate of GTPase activation for G24A tRNA^{Trp} compared to wild-type tRNA^{Trp} that is independent of the presence of mRNA or identity of the near-cognate codon⁷.

The mechanism for miscoding by G24A tRNA^{Trp}

Inspection of the body of G24A tRNA^{Trp} reveals that the G24A mutation promotes miscoding by preferentially stabilizing the distorted conformation through formation of an additional internal interaction. The mutation introduces an exocyclic amine at ring position 6 of nucleotide 24 that, in this distorted A/T state, is within hydrogen bonding distance of the exocyclic O6 of G44 (Fig. 3a). This hydrogen bond, which would not be possible in wild-type tRNA^{Trp} or in the unbent G24A tRNA^{Trp}, could stabilize the bent form of the G24A tRNA^{Trp}. This mutant tRNA is therefore more easily able to adopt the A/T conformation than its wild-type counterpart and thus more easily misreads the code. This 24–44 interaction could only form if residue 24 contains an exocyclic amine at

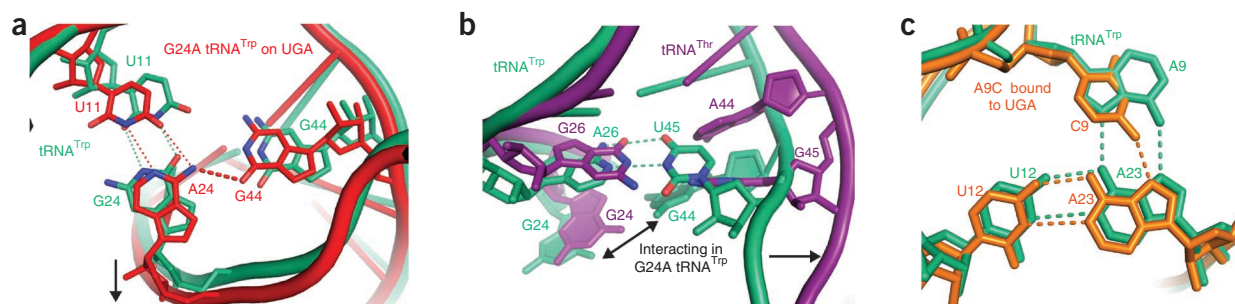


Figure 3 Miscoding by the G24A and A9C Trp-tRNA^{Trp}. (a) Mutation of G24A (red) facilitates formation of a hydrogen bonding interaction that is not possible in native tRNA^{Trp} (green) between the exocyclic amine of A24 and O6 of G44. This interaction is facilitated by a small shift in the RNA backbone between residues 20–30 and a commensurate movement between residues 9–16. (b) The interaction between residues 24 and 44 in the G24A tRNA^{Trp} is only possible because of a base pair between residues A26–U45 in tRNA^{Trp} that dictates the backbone conformation in this region. In contrast, tRNA^{Thr} (purple)¹⁴ contains two purines at these positions—G26 and G45—which push the tRNA backbone apart and separate residues G24 and A44. That the A26–U45 base pair is not conserved in bacterial tRNA^{Trp} further illustrates that evolution has fine-tuned each tRNA to find a unique solution to tRNA bending during decoding. (c) In native tRNA^{Trp} (shown in green), a base triple forms between residues 9:12:23, which is at the junction of three separate strands of the tRNA. Mutation of residue 9 to a cytosine (shown in orange) weakens both the packing and hydrogen-bonding of this base-triple, which could result in higher flexibility of the tRNA body and explain its ability to miscode.

position 6, consistent with the fact that mutations at residues 24 and 11 only cause miscoding when G24 is mutated to an A or C².

It is therefore tempting to predict that in all bacterial species, native tRNA^{Trp} would either not contain an A or C at position 24 or be unable to form a hydrogen bond between residues 24 and 44. Indeed, of ~560 bacterial tRNA^{Trp} sequences, 97.5% would not be able to make this 24–44 hydrogen bond¹⁷. However, the remaining few bacterial tRNA^{Trp} that do contain an A or C at position 24 and a G at position 44 presumably do not miscode. These tRNAs have likely arrived at an energetic balance that includes this hydrogen bond or have positioned residue 44 away from 24 in the A/T conformation.

The structural cause of miscoding by G24A tRNA was not predicted by the many previous biochemical and structural studies, perhaps because nucleotides 44 and 24 are far apart in unbent tRNAs (7.2 Å in yeast tRNA^{Phe} (ref. 18), **Supplementary Fig. 2**), tRNA bound to EF-Tu (7.8 Å)¹⁹, and even in the complex of distorted tRNA^{Thr} bound to the ribosome (8.2 Å¹⁴, **Fig. 3b**). The interaction that causes miscoding is possible only in the bent form of G24A tRNA^{Trp} because this conformation has a base pair between residues A26 and U45 that brings the strands containing G44 and A24 together when tRNA is bound to the ribosome (**Fig. 3b**). Direct observation of this interaction also explains why the strength of the 24:11 base pair does not correlate with miscoding efficiency², an observation that discounts the simple explanation that the G24A mutation increases tRNA flexibility, consistent with recent biochemical work⁵.

tRNA identity affects the tRNA conformation in the A/T state

In our previously reported structure of 70S-EF-Tu-Thr-tRNA^{Thr}, the tRNA^{Thr} contains guanosines at both positions 26 and 45. Comparing this structure with the structure containing Trp-tRNA^{Trp}, one of the most obvious differences is at nucleotides 44–45, which in Thr-tRNA^{Thr} are pushed away from the tRNA body but in Trp-tRNA^{Trp} are drawn in by more than 5 Å owing to the contacts between 45 and 26 (**Fig. 3b**). The overall bends in the two tRNAs are extremely similar, and the respective positions of the tRNA-EF-Tu interface are within approximately 1 Å of each other. To accommodate a larger amino acid, the backbone of EF-Tu around the amino acid binding pocket and the 3' end of the Trp-tRNA^{Trp} have shifted very slightly. These small differences, seen in both the structures reported here and the ribosome-EF-Tu-GDP-PCP-Trp-tRNA^{Trp} structure¹³, are compensated for by slight rotations in EF-Tu of domain 1 with respect to domains 2 and 3 (**Supplementary Fig. 3**), allowing EF-Tu to interact with the ribosome in the same way, regardless of tRNA identity. Similar small differences in the conformation of tRNA and EF-Tu during decoding have been reported from low-resolution studies²⁰. These subtle differences in tRNA conformation on the ribosome are understandable given that tRNAs have differences in sequence and structure that are required for fidelity of other processes such as aminoacylation.

Miscoding by A9C tRNA^{Trp}

From the structure of A9C tRNA, it seems evident that its error-prone phenotype is due to enhanced flexibility of the tRNA, which facilitates formation of the A/T conformation. Adenosine 9 in tRNA^{Trp} forms a *trans*-Hoogsteen-Hoogsteen base pair²¹ with A23 of the A23-U12 pair in the D-stem. This base triple is at the junction between three separate strands of the tRNA and is within the upper region of distortion of the A/T conformation. Mutation of A9 to cytosine weakens this triple, which leads to the destabilization of the tRNA (**Fig. 3c**). Indeed, the electron density for regions of this tRNA body is considerably weaker when compared to that for other structures, or even to the anticodon and 3' end of the A9C tRNA. This enhanced flexibility would allow

A9C tRNA to more easily access the A/T state and position EF-Tu in conformation for GTP hydrolysis even in the presence of the UGA stop codon. This increase in flexibility is likely sufficient to explain the ~18-fold increase in misreading that has been reported².

Proper decoding by the ribosome requires a delicate balance between the energy derived from binding of a cognate tRNA and the combined energy required for distortions in the tRNA, EF-Tu and the 30S subunit that enable GTP hydrolysis. The two mutant tRNAs studied here cause miscoding through different mechanisms: A9C by increasing flexibility and G24A by facilitating an additional internal interaction. Using these strategies, the G24A and A9C mutations decrease the energetic penalty for tRNA distortion into the A/T state, which allows GTPase activation to occur on the near-cognate UGA stop codon. Comparison of Trp-tRNA^{Trp} and Thr-tRNA^{Thr} suggest that the exact details of the decoding conformations will be different for every tRNA, as the energetics of the tRNA body have been uniquely optimized to ensure accurate decoding while maintaining requirements for other processes such as aminoacylation and a uniform affinity for EF-Tu²². Any perturbation to the precise energetic balance in the tRNA, EF-Tu and the ribosome can therefore lead to hyperaccuracy or miscoding.

METHODS

Methods and any associated references are available in the online version of the paper at <http://www.nature.com/nsmb/>.

Accession codes. Protein Data Bank: 2Y0U, 2Y0V, 2Y0W, 2Y0X for A9C; 2Y0Y, 2Y0Z, 2Y12, 2Y13 for HS; 2Y14, 2Y15, 2Y16, 2Y17 for HT; and 2Y18, 2Y19, 2Y10, 2Y11 for TT.

Note: Supplementary information is available on the Nature Structural & Molecular Biology website.

ACKNOWLEDGMENTS

We thank R. Green and R. Ortiz-Meoz, Johns Hopkins University, for plasmids and bacterial strains for production of mutant tRNA^{Trp}, A. McCarthy and S. Brockhauser at ESRF ID14.4 for facilitating data collection, O. Uhlenbeck for helpful discussion and F. Murphy for scripting. This work was supported by the Medical Research Council, the Wellcome Trust, the Agouron Institute and the Louis-Jeantet Foundation. R.M.V. received support from the Gates-Cambridge scholarship. T.M.S. received support from the Human Frontier Science Program and Emmanuel College.

AUTHOR CONTRIBUTIONS

T.M.S. and R.M.V. designed the experiments, prepared and crystallized the ribosomal complexes, collected and processed X-ray crystallography data, determined, refined and analyzed the structures, and prepared the manuscript and figures. A.C.K. purified macromolecular components, prepared and crystallized ribosomal complexes and aided with collection of X-ray crystallography data. V.R. suggested the study and provided intellectual input and supervision.

COMPETING FINANCIAL INTERESTS

The authors declare competing financial interests: details accompany the full-text HTML version of the paper at <http://www.nature.com/nsmb/>.

Published online at <http://www.nature.com/nsmb/>.

Reprints and permissions information is available online at <http://npg.nature.com/reprintsandpermissions/>.

- Hirsh, D. Tryptophan tRNA of *Escherichia coli*. *Nature* **228**, 57 (1970).
- Smith, D. & Yarus, M. Transfer RNA structure and coding specificity. II. A D-arm tertiary interaction that restricts coding range. *J. Mol. Biol.* **206**, 503–511 (1989).
- Smith, D. & Yarus, M. Transfer RNA structure and coding specificity. I. Evidence that a D-arm mutation reduces tRNA dissociation from the ribosome. *J. Mol. Biol.* **206**, 489–501 (1989).
- Schultz, D.W. & Yarus, M. tRNA structure and ribosomal function. I. tRNA nucleotide 27–43 mutations enhance first position wobble. *J. Mol. Biol.* **235**, 1381–1394 (1994).

5. Ortiz-Meoz, R.F. & Green, R. Functional elucidation of a key contact between tRNA and the large ribosomal subunit rRNA during decoding. *RNA* **16**, 2002–2013 (2010).
6. Favre, A., Buchingham, R. & Thomas, G. tRNA tertiary structure in solution as probed by the photochemically induced 8–13 cross-link. *Nucleic Acids Res.* **2**, 1421–1431 (1975).
7. Cochella, L. & Green, R. An active role for tRNA in decoding beyond codon:anticodon pairing. *Science* **308**, 1178–1180 (2005).
8. Ogle, J.M. *et al.* Recognition of cognate transfer RNA by the 30S ribosomal subunit. *Science* **292**, 897–902 (2001).
9. Agris, P.F., Vendeix, F.A. & Graham, W.D. tRNA's wobble decoding of the genome: 40 years of modification. *J. Mol. Biol.* **366**, 1–13 (2007).
10. Pape, T., Wintermeyer, W. & Rodnina, M. Induced fit in initial selection and proofreading of aminoacyl-tRNA on the ribosome. *EMBO J.* **18**, 3800–3807 (1999).
11. Parker, J. Errors and alternatives in reading the universal genetic code. *Microbiol. Rev.* **53**, 273–298 (1989).
12. Fersht, A.R. The hydrogen bond in molecular recognition. *Trends Biochem. Sci.* **12**, 301–304 (1987).
13. Voorhees, R.M., Schmeing, T.M., Kelley, A.C. & Ramakrishnan, V. The mechanism for activation of GTP hydrolysis on the ribosome. *Science* **330**, 835–838 (2010).
14. Schmeing, T.M. *et al.* The crystal structure of the ribosome bound to EF-Tu and aminoacyl-tRNA. *Science* **326**, 688–694 (2009).
15. Murphy, F.V., Ramakrishnan, V., Malkiewicz, A. & Agris, P.F. The role of modifications in codon discrimination by tRNA^{Lys}_{UUU}. *Nat. Struct. Mol. Biol.* **11**, 1186–1191 (2004).
16. Olejniczak, M. & Uhlenbeck, O.C. tRNA residues that have coevolved with their anticodon to ensure uniform and accurate codon recognition. *Biochimie* **88**, 943–950 (2006).
17. Lowe, T.M. & Eddy, S.R. tRNAscan-SE: a program for improved detection of transfer RNA genes in genomic sequence. *Nucleic Acids Res.* **25**, 955–964 (1997).
18. Shi, H. & Moore, P.B. The crystal structure of yeast phenylalanine tRNA at 1.93 Å resolution: a classic structure revisited. *RNA* **6**, 1091–1105 (2000).
19. Nissen, P. *et al.* Crystal structure of the ternary complex of Phe-tRNA_{Phe}, EF-Tu, and a GTP analog. *Science* **270**, 1464–1472 (1995).
20. Li, W. *et al.* Recognition of aminoacyl-tRNA: a common molecular mechanism revealed by cryo-EM. *EMBO J.* **27**, 3322–3331 (2008).
21. Leontis, N.B. & Westhof, E. Geometric nomenclature and classification of RNA base pairs. *RNA* **7**, 499–512 (2001).
22. Fahlman, R.P., Dale, T. & Uhlenbeck, O.C. Uniform binding of aminoacylated transfer RNAs to the ribosomal A and P sites. *Mol. Cell* **16**, 799–805 (2004).

ONLINE METHODS

***Thermus thermophilus*.** 70S ribosomes harboring a C-terminal truncation of protein L9 (ref. 23) were purified as previously described²⁴ from cells grown at the Bioexpression and Fermentation Facility at the University of Georgia. Model mRNAs were purchased from Dharmacon (Thermo Scientific) with the following sequences: cognate tryptophan mRNA, 5'-GGCAAGGAGGUAAAAAUGUUCUGGAAA-3'; UGA stop mRNA, 5'-GGCAAGGAGGUAAAAAUGUUCUGAAA-3'.

tRNA expression and purification. Wild-type tRNA^{Trp} was expressed as described for tRNA^{Phe} (ref. 24). Plasmid pRT33C and strain MY87 for expression of Hirsh tRNA^{7,25} was a kind gift from R. Green. Quikchange mutagenesis (Agilent) was done to obtain a tRNA^{Trp} with an A9C mutation. Hirsh tRNA and A9C tRNA were expressed as described⁷.

The mutant and wild-type tRNA^{Trp} were phenol extracted from lysed cells as described for tRNA^{Phe} (ref. 24). Extracted tRNA was bound to a DEAE-Sepharose column equilibrated in 50 mM Tris-HCl, pH 7.5, and eluted with a linear gradient to 50 mM Tris-HCl, pH 7.5, and 1 M NaCl buffer over 5 column volumes. Fractions containing tRNA were pooled and solid (NH₄)₂SO₄ was added to a final concentration of 1.7 M, for loading onto a TSK 5PW hydrophobic column equilibrated in 10 mM ammonium acetate, pH 6.3, 1.7 M (NH₄)₂SO₄. tRNA was eluted using a linear gradient 1.7–0.85 M (NH₄)₂SO₄ over 5 column volumes. tRNA from the resulting peak fractions were assayed for aminoacylation efficiency using [¹⁴C]tryptophan as described⁷.

The tRNA from the appropriate fractions was further purified using a C4 reverse-phase column equilibrated in 20 mM NH₄OAc, pH 5.5, 400 mM NaCl, 10 mM Mg(OAc)₂, eluted with a 0–40% linear gradient over 8 column volumes using the same buffer containing 60% methanol, then aminoacylated with non-radioactive tryptophan. Separation of acylated from deacylated tRNA was accomplished using the TSK 5PW hydrophobic column using the same conditions described above. The sample was dialyzed into a solution of 10 mM NH₄OAc, pH 5, 50 mM KCl and stored at –80 °C.

Complex formation. Complexes of Trp-tRNA^{Trp}-GTP-70S ribosome were prepared and purified by Ni-NTA affinity purification as described¹⁴, with the

exception that the tRNA was pre-acylated before complex formation and the antibiotic paromomycin was not included in the reaction mixture. Paromomycin increases miscoding and was therefore not appropriate for the present study with noncognate tRNA. However, we observed no notable differences in the cognate tRNA^{Trp} and tRNA^{Thr} complexes attributable to paromomycin.

Affinity purification for complexes containing Trp-tRNA^{Trp} and Hirsh tRNA bound to a cognate UGG codon both resulted in 45–55% yield of input ribosomes. Complexes with Hirsh tRNA and an mRNA containing a near-cognate UGA stop codon were somewhat lower, at ~20% yield. Control experiments with Trp-tRNA^{Trp} and UGA were very low, at ~3% yield.

Crystallization. Crystals were grown under conditions described¹⁴, with the reservoir solution modified to include 5.3% PEG 5.2 and 60–100 mM KCl. Data were collected at beamline ID 14–4 of the European Synchrotron Light Source²⁶ and processed as described¹⁴ using XDS²⁷. Iterative rounds of model building and refinement were carried out in Coot²⁸ and CNS²⁹ as previously described¹⁴. Sequence analysis of residues 24 and 44 in bacterial tRNA^{Trp} was done on sequences obtained from the Genomic tRNA Database¹⁷. All figures were made in PyMOL (DeLano Scientific).

23. Gao, Y.G. *et al.* The structure of the ribosome with elongation factor G trapped in the posttranslocational state. *Science* **326**, 694–699 (2009).
24. Selmer, M. *et al.* Structure of the 70S ribosome complexed with mRNA and tRNA. *Science* **313**, 1935–1942 (2006).
25. Eisenberg, S.P., Söll, L. & Yarus, M. The purification and sequence of a temperature-sensitive tryptophan tRNA. *J. Biol. Chem.* **254**, 5562–5566 (1979).
26. McCarthy, A.A. *et al.* A decade of user operation on the macromolecular crystallography MAD beamline ID14–4 at the ESRF. *J. Synchrotron Radiat.* **16**, 803–812 (2009).
27. Kabsch, W. Automatic processing of rotation diffraction data from crystals of initially unknown symmetry and cell constants. *J. Appl. Crystallogr.* **26**, 795–800 (1993).
28. Emsley, P. & Cowtan, K. Coot: model-building tools for molecular graphics. *Acta Crystallogr. D Biol. Crystallogr.* **60**, 2126–2132 (2004).
29. Brünger, A.T. *et al.* Crystallography & NMR system: a new software suite for macromolecular structure determination. *Acta Crystallogr. D Biol. Crystallogr.* **54**, 905–921 (1998).